Intracavity Raman Scattering from Molecular Beams: Direct Determination of Local Properties in an Expanding Jet Beam

Silvera, I.F.; Tommasini, F.

Published in:
Physical Review Letters

DOI:
10.1103/PhysRevLett.37.136

even though it does depend to some extent on the assumed spin for ^{69}Se. Our derived values of a for ^{69}As compare favorably with the prescriptions of Ref. 7 and with results similarly derived from blocking measurements[11] on ^{71}As and ^{73}As: in all cases $a \sim 11$ MeV^{-1}. By comparison, the width Γ_γ, quoted in Table I for an excitation energy of 4.75 MeV (the region in which the proton spectrum is most sensitive to Γ_γ), is higher by a factor of 5 than the simple $E1$ predictions, but such a value is still consistent with known γ widths in the same mass region.

Evidently, the calculated energy dependence of the proton spectrum and level lifetimes is in reasonable agreement with the average behavior of the data (Fig. 1) although there may be an indication of significant upward fluctuations from the average at low energy particularly in the lifetime data. This suggests strongly favored proton decay in this region, a possibility that needs to be studied in future experiments with improved counting statistics. It is such features of this and other proton-emitting nuclei that are now made accessible through the new p-x technique of lifetime measurement.

We should like to thank Dr. P. G. Hansen for a valuable discussion. Two of us (E. T. H. C. and K. P. J.) gratefully acknowledge the hospitality of Atomic Energy of Canada Limited.

*Present address: TRIUMF, Vancouver, B. C., Canada.

†Work supported by a grant from the National Research Council of Canada.

[1]D. B. Fossan and E. K. Warburton, in *Nuclear Spectroscopy and Reactions*, edited by J. Cerny (Academic, New York, 1974), Pt. C, pp. 307–374.

[2]K. D. Sevier, *Low Energy Electron Spectrometry* (Wiley-Interscience, New York, 1972), pp. 220–241.

[3]O. Keski-Rahkonen and M. O. Krause, At. Data Nucl. Data 14, 139 (1974).

[4]J. C. Hardy, in *Nuclear Spectroscopy and Reactions*, edited by J. Cerny (Academic, New York, 1974), Pt. C, pp. 417–466.

[5]J. H. Hsu, R. Fournier, B. Hird, J. Kroon, G. C. Ball, and F. Ingebretsen, Nucl. Phys. A179, 80 (1972); note that the ^{68}Ge mass quoted by A. H. Wapstra and N. B. Gove [Nucl. Data 9, 267 (1971)], is based on a typographical error.

[6]K. Takahashi, M. Yamada, and T. Kondoh, At. Data Nucl. Data 12, 101 (1973).

[7]A. Gilbert and A. G. W. Cameron, Can. J. Phys. 43, 1446 (1965); J. W. Truran, A. G. W. Cameron, and E. Hilf, CERN Report No. 70-30, 1970 (unpublished), p. 275.

[8]G. A. Bartholomew, E. D. Earle, A. J. Ferguson, J. W. Knowles, and M. A. Lone, in *Advances in Nuclear Physics*, edited by M. Baranger and E. Vogt (Plenum, New York, 1973), Vol. 7, pp. 229–324.

[9]G. S. Mani, M. A. Melkanoff, and I. Iori, Centre d'Etudes Nucléaires de Saclay Report No. CEA-2379 (unpublished).

[10]E. Nolte, Y. Shida, W. Kutschera, R. Prestele, and H. Morinaga, Z. Phys. 268, 267 (1974).

[11]G. J. Clark, J. M. Poate, E. Fuschini, C. Maroni, I. G. Massa, A. Uguzzoni, and E. Verondini, Nucl. Phys. A173, 73 (1971).

Intracavity Raman Scattering from Molecular Beams: Direct Determination of Local Properties in an Expanding Jet Beam

Isaac F. Silvera and F. Tommasini*
Natuurkundig Laboratorium, Universiteit van Amsterdam, Amsterdam-C, Netherlands
(Received 28 May 1976)

An intracavity crossed laser-beam, molecular-jet-beam system has been developed for studying the properties of expanding jet beams by means of light scattering. Raman scattering has been used to measure the local rotational temperature and absolute density of monomers in a jet beam of CO_2 as a function of axial distance from the nozzle. A well-defined rotational temperature has been observed. This temperature drops rapidly for distances of a few nozzle diameters in agreement with isentropic theory and thereafter remains roughly constant.

We have developed a crossed laser-beam, molecular-jet-beam system for studies of the latter by means of light scattering. The jet beam intersects the sharply focused laser beam within the laser cavity providing a high-sensitivity, high-resolution system which does not disturb beam properties. The rotational and vibrational temperatures and absolute monomer density of a molecular jet beam can be measured directly as a function of position relative to the nozzle with an axial resolution of $\simeq 10$ μm. In addition the method is potentially capable of observing the

spectra of clusters which would provide useful information on interatomic or intermolecular potentials. In this Letter we discuss the application of this technique to the study of an expanding CO_2 jet, also studied by Lewis, Williams, and Powell,[1] to measure directly the rotational temperature and monomer density as a function of the axial distance x from the nozzle.

The apparatus is shown schematically[2] in Fig. 1 and consists of a laser beam and jet beam whose axes cross at right angles. In the geometry shown the right-angle Raman-scattered light emerging from the focal region of the laser is imaged on the slit of a Spex 1401 spectrometer after being rotated 90° by means of a dove prism. Raman signals are proportional to the density of scatterers in the jet beam and to the laser power. In order to study weakly scattering or low-density jet beams the laser cavity was built around the jet.[3] The laser system consisted of a Spectra Physics argon-ion laser whose output mirror M_2 could be removed and replaced by the 20-mm focal-length lens L and the 99.8% reflecting mirror M_3 so that the laser was focused within the cavity to a region of width $\simeq 10\ \mu$m and length $\simeq 300\ \mu$m. The scattered-light signal is enhanced both by the focusing and by the increased power within the cavity. The output power of the laser operating in the normal mode is about 1.5 W at 5145 Å whereas the maximum power we have obtained in the extended cavity mode is $\simeq 25$ W. A substantially higher cavity power was expected; however, we have not as yet pursued the source of cavity loss that is limiting the power. In this situation it has been convenient to leave the laser-output mirror M_2 installed and work in a coupled-cavity mode with a power in the jet cavity of 10–20 W. After alignment, the carefully designed mechanical mounting was stable for days. The laser power could be photometrically stabilized to better than 1%.

The jet was produced by means of a sonic nozzle (diameters D of 0.1 and 0.2 mm were used)

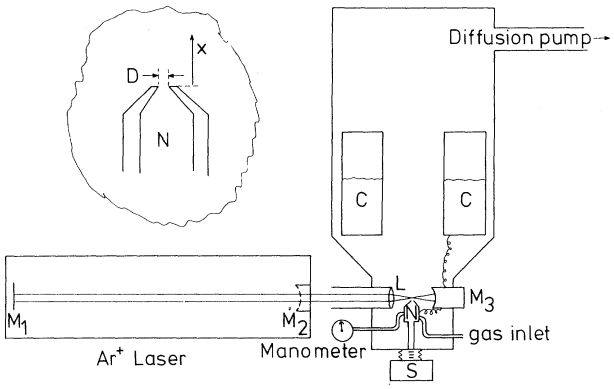

FIG. 1. Schematic diagram of the experimental arrangement described in the text. The light-collection optics, normal to the plane of the figure, are omitted here. The nozzle shape is shown in the inset.

that could be translated vertically to vary the axial distance of the nozzle from the scattering region over a distance of 4 mm with a resolution of a few microns. In addition the nozzle could be translated with two degrees of freedom, perpendicular to the jet axis, so that the jet and laser beam intersected at the laser focus. In practice the minimum distance x was $\simeq 40\ \mu$m; smaller distances resulted in interference between the nozzle and the laser-cavity mode. The nozzle temperature was measured with a thermocouple and controlled by means of a resistance heater and a thermal link to the cryogenic liquid. Stagnation temperatures from somewhat higher than that of the cryogen up to ~450 K could be achieved.

The gas from the nozzle was directed at a cold surface C which provided a cryogenic pumping speed of $\simeq 5000$ l/sec (CO_2 gas with liquid-nitrogen cryogen) as determined from consideration of nozzle flow and pressure in the chamber. A small diffusion pump served to prepump the system. A skimmer was not used.

The pure rotational-Raman-scattering efficiency (the fraction of incident light scattered per unit frequency per unit solid angle per unit length of the sample) is given by[4]

$$I(J\to J') = r\frac{\nu\nu'^3}{c^4}(\alpha_\parallel-\alpha_\perp)^2\rho_1\frac{S_J\exp(-E_J/KT_R)}{\sum_{\text{even } J}(2J+1)\exp(-E_J/KT_R)}, \tag{1a}$$

with

$$S_J=\frac{3(J+1)(J+2)}{2(2J+3)},\quad J\to J+2\ \text{(Stokes)}, \tag{1b}$$

$$=\frac{3J(J-1)}{2(2J-1)},\quad J\to J-2\ \text{(anti-Stokes)}. \tag{1c}$$

Here ν is the frequency of the incident light and ν' the scattered light; $(\alpha_\parallel-\alpha_\perp)$ is the anisotropy of the polarizability, ρ_1 is the number of density of isolated CO_2 scatters, J is the rotational quantum number of the initial state, and T_R is the ro-

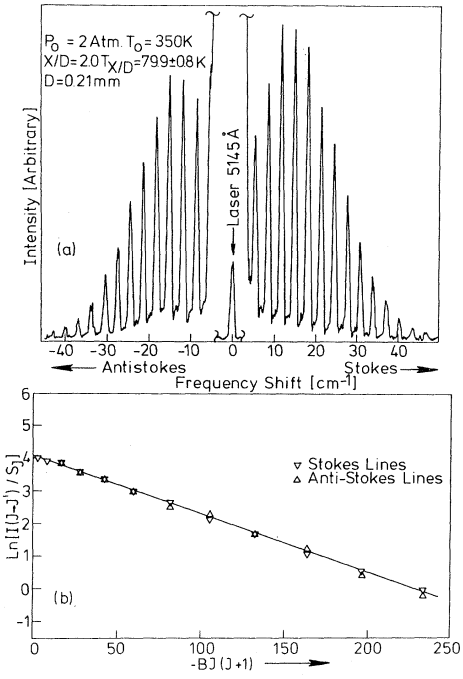

FIG. 2. (a) The pure-rotational Raman spectrum of CO_2 in a jet beam. The broad bump underlying in the background at -15 cm^{-1} is an instrumental effect. (b) Linearized display of the data showing that the spectrum can be locally characterized by an equilibrium rotational temperature. The fit clearly shows that Stokes and anti-Stokes transitions provide redundant information.

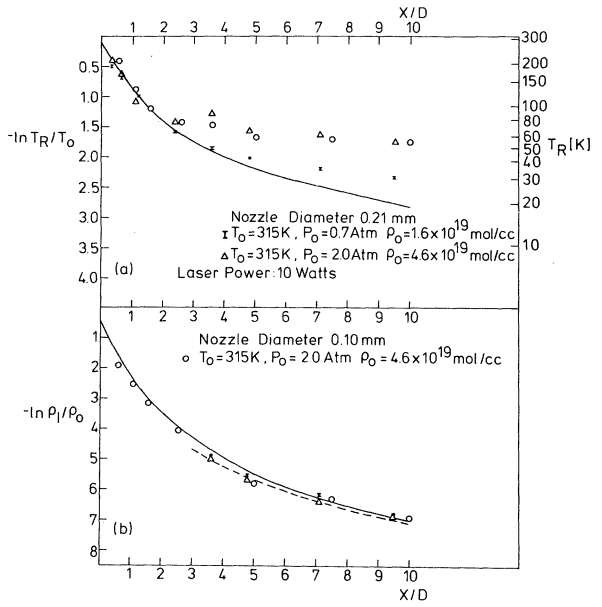

FIG. 3. Semilogarithmic plot of the axial temperature and density dependence of an expanding CO_2 jet beam. The solid lines are theoretical curves for an isentropic expansion. The broken line shows the $(x/D)^{-2}$ dependence of density and is displaced from the isentropic expansion curve for clarity. The absolute temperature is given on the right-hand scale. The error bars as defined in the text are shown for the $P_0 = 0.7$ atm data. Data points for $x/D < 3$ are not shown in (b) for the 0.21-mm nozzle as an aperture required at these distances to prevent a geometric filling error was improperly set.

tational temperature. In CO_2, to a good approximation, $E_J = BJ(J+1)$ with $B = 0.390\,27$ cm^{-1} [5]; the value 2.1×10^{-24} cm^3 is assumed for $\alpha_\parallel - \alpha_\perp$.[6] The sum over states is restricted to even J by spin statistics (if the molecules are in their ground vibrational states). r is a numerical factor which, among other constants, includes the polarization dependence which is not indexed in Eq. (1a).

A typical rotational-Raman-scattering spectrum from the jet is shown in Fig. 2(a). To determine both temperature and density from Eq. (1a), we plot [Fig. 2(b)] the logarithm of the measured peak intensity divided by S_J versus $-BJ(J+1)$ so that the slope of the least-squares straight-line fit is proportional to T_R^{-1} and the intercept to ρ_1. The absolute density was determined by comparison to a reference spectrum of nonflowing CO_2 gas at a known pressure in the scattering chamber. Since a jet beam is a thermodynamic nonequilibrium system, it is not *a priori* evident that the spectra must fit Eq. (1a), the distribution for an equilibrium gas.[7] We have been able to fit all spectra (a few hundred) to a straight line as in Fig. 2(b) with no significant systematic deviation. We thus assume that the rotational temperature T_R that we have measured is a meaningful quantity within the scattering region.

The results of the data analyses for a few different nozzle stagnation conditions and two nozzle diameters are plotted in Figs. 3(a) and 3(b). The error bars represent a standard deviation as determined from the least-squares fits as in Fig. 2(b). The temperature and density fall dramatically within a few nozzle diameters downstream from the nozzle. In Fig. 3 we compare the measured results to the theoretical curves for an isentropic expansion[8] in which all degrees of freedom are in thermodynamic equilibrium:

$$T/T_0 = [1 + M^2(\gamma - 1)/2]^{-1}, \tag{2}$$

$$\rho/\rho_0 = [1 + M^2(\gamma - 1)/2]^{1/(1-\gamma)}. \tag{3}$$

Here γ is the specific-heat ratio C_p/C_v taken to

be $\frac{7}{5}$ for CO_2. The axial dependence of the Mach number M was determined from the graph of Owen and Thornhill.[9,8] A fairly accurate analytic axial dependence can be obtained by using the fitting formula of Ashkenas and Sherman[10] in Eqs. (2) and (3):

$$M = A[(x - x_0)/D]^{\gamma-1} - \frac{\frac{1}{2}[(\gamma+1)/(\gamma-1)]}{A[(x-x_0)/D]^{\gamma-1}}, \qquad (4)$$

with $A = 3.65$ and $x_0/D = 0.40$. In the data shown, the temperature appears to fit the theoretical curve reasonably well until $x/D \sim 2$–3, then deviates, approaching some constant value which was found to be between ~25 and 50 K for various runs in which T_0 was varied from 210 to 423 K, P_0 from 0.3 to 2.0 atm, and x/D from ~0.5 to 30. For the lowest stagnation temperature, high-flow runs, deviations began for $x/D < 1$ whereas for a high-temperature, lower-flow run, the curve was followed to $x/D \simeq 10$ (data not shown). We consider this onset of deviation to be the region where the rotational and translational degrees of freedom go out of equilibrium. For a given temperature, the lower the density the lower the collision rate. However, for a given stagnation temperature, the lower-stagnation-pressure runs follow the isentrope to large x/D values, implying that contrary to expectation the onset of deviation is not controlled in this case by the decrease of the collision rate. This behavior could be a result of condensation in the beam.[11]

The density agrees quite well with the theoretical curve, even beyond the point where the temperature deviates. In the crossover from an isentropic to a free expansion, the density fall-off goes over into an inverse quadratic behavior. For $x/D \gtrsim 3$ and in the absence of condensation the isentropic and free-expansion behavior are difficult to distinguish experimentally. On this basis it is not possible to characterize the phenomena in this region. Condensation or formation of clusters[11] is expected to cause the density to deviate below the theoretical curve. Van Deursen, Van Lumig, and Reuss[12] have shown that there is a critical stagnation pressure P_L above which monomer concentration remains roughly constant with increasing pressure as large clusters begin to form. In CO_2 the pure-rotational Raman scattering as shown in Fig. 2(a) should arise only from monomers. The anisotropic pair interactions in a cluster are large compared to the free-molecule rotational splittings and thus should suppress or greatly modify the rotational scattering[13] so that clustered molecules do not contribute to the measured intensity (and thus the measured density) in the spectral region under study. For the $D = 0.10$-mm nozzle and in the region $1 < x/D < 10$ we have measured the density for pressures bracketing P_L (scaled to our conditions[14]) and do not find a significant deviation from linear behavior, implying that the clustering observed by Van Deursen, Van Lumig, and Reuss takes place further downstream. We note that Lewis, Williams, and Powell[1] have demonstrated the onset of clustering by means of Rayleigh scattering in the vicinity of the nozzle, with, however, a substantially larger nozzle diameter than ours.

For higher-nozzle-flow conditions, bumps have been observed in both T and ρ_1 as a function of x/D. Further work is underway to study the systematics, clustering, and to measure directly the local vibrational and translational temperatures by means of light scattering.

We would like to thank R. J. Wijngaarden for aid with measurements and data analyses. We also acknowledge useful discussions with A. J. Berlinsky, J. Reuss, and L. Van Deursen.

---

*Permanent address: Istituto di Scienze Fisiche, Università di Genova, Genova, Italy.

[1]J. W. L. Lewis, W. D. Williams, and H. M. Powell, in *Ninth International Symposium on Rarefied Gas Dynamics, Gottingham, West Germany, 1974*, edited by M. Becker and M. Fiebig (Deutsche Forschungs- und Versuchsantalt für Luft- und Raumfahrt, Freiburg, 1974), Vol. 2.

[2]A detailed description of the apparatus will be given elsewhere by the authors.

[3]For a discussion of intracavity light scattering see, for example, J. J. Barrett and N. I. Adams, III, J. Opt. Soc. Am. 58, 311 (1968); S. Brodersen and J. Bendtser, J. Raman Spectrosc. 1, 97 (1973).

[4]G. Herzberg, *Spectra of Diatomic Molecules* (Van Nostrand Reinhold, New York, 1950), 2nd ed., p. 127.

[5]J. J. Barrett and A. Weber, J. Opt. Soc. Am. 60, 70 (1970).

[6]J. O. Hirschfelder, C. F. Curtis, and R. B. Bird, *Molecular Theory of Gases and Liquids* (Wiley, New York, 1964), p. 950.

[7]S. G. Kukolich, D. E. Oates, and J. H. S. Wang, J. Chem. Phys. 61, 4686 (1974).

[8]See for example the review article by J. B. Anderson, in *Molecular Beams and Low Density Gas Dynamics*, edited by P. P. Wegener (Dekker, New York, 1974), Chap. I, and references therein.

[9]P. L. Owen and C. K. Thornhill, Aeronautics Research Council (U.K.) Research Memorandum No. 2616, 1948 (unpublished).

[10]H. Ashkenas and F. S. Sherman, in *Fourth Interna-*

tional Symposium on Rarefied Gas Dynamics, edited by J. H. de Leeuw (Academic, New York, 1966), Vol. 2, p. 84.

[11]See for example the review article by O. F. Hagena, in *Molecular Beams and Low Density Gas Dynamics*, edited by P. P. Wegener (Dekker, New York, 1974), Chap. 2; O. F. Hagena and W. Obert, J. Chem. Phys. 56, 1793 (1972).

[12]A. Van Deursen, A. Van Lumig, and J. Reuss, Int. J. Mass. Spectrom. Ion Phys. 18, 129 (1975).

[13]I. F. Silvera and P. J. Berkhout, in *Proceedings of the Third International Conference on Light Scattering in Solids*, Campinas, Brazil, 1975, edited by M. Balkanski, R. Leite, and S. P. S. Porto (Flammarion, Paris, 1976), p. 742.

[14]A. Van Deursen, private communication.

Relaxation Instability in Tokamaks

A. Sykes and J. A. Wesson
Culham Laboratory, Abingdon, Oxon, United Kingdom
(Received 12 April 1976)

A three-dimensional, nonlinear, numerical simulation is described in which saw-tooth oscillations occur as a result of a hydromagnetic relaxation instability. The time evolution of the magnetic topology demonstrates the essential validity of the model suggested by Kadomtsev to explain the saw-tooth oscillations observed in tokamak experiments.

Several tokamak experiments have exhibited an unstable behavior having the form of relaxation oscillations in which the soft-x-ray emission has a saw-tooth time dependence[1,2,3]. In the central region the results indicate a slowly rising temperature followed by a rapid fall. The whole process occurs repeatedly with a period of the order of a millisecond.

The following general explanation of this behavior has gained some acceptance. The inner temperature rises due to Ohmic heating. The resulting increase in conductivity leads to an increase in the current density on axis and as a consequence the safety factor q falls below unity. The plasma then undergoes an instability which transports the energy which has been produced by Ohmic heating out to larger radii. In some way the plasma relaxes back to an axisymmetric state having $q>1$ and the whole process is then repeated.

The question arises as to precisely how this phenomenon occurs. A model has been suggested by Kadomtsev,[4] the basic elements of which are as follows. When the value of q falls below unity an $m=1$ instability occurs. As a result the plasma surfaces are displaced to one side and resistivity allows a magnetic island to form on the opposite side of the plasma around the $q=1$ surface. This island grows and displaces the original set of magnetic surfaces which then decay away. The resulting value of q is greater than unity but the concentration of the current toward the magnetic axis leads to a lowering of q until instability reappears and the whole cycle is repeated.

Our purpose here is to describe the results of a three-dimensional, nonlinear calculation which reproduces relaxation instabilities of the type observed experimentally and which demonstrates the basic features of Kadomtsev's model. The configuration studied is cylindrical and, in order to achieve acceptable computation times, a higher value of β has been used than is obtained in tokamak experiments.

The equations solved are the time-dependent hydromagnetic equations including resistivity, viscosity, Ohmic heating, and an energy loss. The resistivity is taken to be proportional to $T_e^{-3/2}$. The viscosity used is small and is taken to be constant. The Ohm's law is

$$\vec{E}+\vec{v}\times\vec{B}=\eta(T)\vec{j},$$

and the resulting Ohmic heating is included together with an energy-loss term in the energy equation

$$\frac{1}{\gamma-1}\frac{\partial p}{\partial t}=\frac{1}{\gamma-1}\nabla\cdot(p\vec{v})-p\nabla\cdot\vec{v}+\eta j^2-\frac{1}{\gamma-1}\frac{p}{\tau(x)}.$$

The form of the energy-loss term is arbitrary but it represents an attempt to describe the more rapid energy-loss rate in the outer region.

The calculations were carried out on a rectangular grid using a generalized form of the Lax-Wendroff method. Relaxation oscillations were first demonstrated on a $10\times10\times7$ grid. The calculations described here were carried out on a more refined $14\times14\times10$ grid and showed the